atoms

MDPI

Article

Deep Minima in the Triply Differential Cross Section for Ionization of Atomic Hydrogen by Electron and Positron Impact

C. M. DeMars [1], S. J. Ward [1,*], J. Colgan [2], S. Amami [3] and D. H. Madison [3]

1 Department of Physics, University of North Texas, Denton, TX 76203, USA; CodyDeMars@my.unt.edu
2 Theoretical Division, Los Alamos National Laboratory, Los Alamos, NM 87545, USA; jcolgan@lanl.gov
3 Department of Physics, Missouri University of Science and Technology, Rolla, MI 65409, USA; samc5@mst.edu (S.A.); madison@mst.edu (D.H.M.)
* Correspondence: Sandra.Quintanilla@unt.edu

Received: 06 May 2020; Accepted: 25 May 2020; Published: 29 May 2020

Abstract: We investigate ionization of atomic hydrogen by electron- and positron-impact. We apply the Coulomb–Born (CB1) approximation, various modified CB1 approximations, the three body distorted wave (3DW) approximation, and the time-dependent close-coupling (TDCC) method to electron-impact ionization of hydrogen. For electron-impact ionization of hydrogen for an incident energy of approximately 76.45 eV, we obtain a deep minimum in the CB1 triply differential cross section (TDCS). However, the TDCC for 74.45 eV and the 3DW for 74.46 eV gave a dip in the TDCS. For positron-hydrogen ionization (breakup) we apply the CB1 approximation and a modified CB1 approximation. We obtain a deep minimum in the TDCS and a zero in the CB1 transition matrix element for an incident energy of 100 eV with a gun angle of 56.13°. Corresponding to a zero in the CB1 transition matrix element, there is a vortex in the velocity field associated with this element. For both electron- and positron-impact ionization of hydrogen the velocity field rotates in the same direction, which is anticlockwise. All calculations are performed for a doubly symmetric geometry; the electron-impact ionization is in-plane and the positron-impact ionization is out-of-plane.

Keywords: electron-impact ionization; hydrogen; positron-impact ionization; velocity field; vortices

1. Introduction

Studies of the angular distributions of ionized atomic electrons by charged-particle impact is a rich field that has long been studied due to its importance to other areas of physics (e.g., plasma, medical physics) and also due to the information that is available about the correlated nature of the particle interactions.

It was thought that structures in differential cross sections of atoms by the impact of fast bare charged particles could be described by using the first and second Born terms [1]. However, as discussed by Berakdar and Briggs [2] the deep minimum observed in the experimentally measured triply differential cross section (TDCS) of helium [3,4] is a different feature to those structures reported in reference [1]. Interestingly, Macek et al. [5] showed that a zero in the ionization element and the TDCS obtained using the theory of reference [2,6] corresponds to a vortex in the velocity field associated with this element.

Berakdar and Briggs [2] for electron-impact ionization of helium used the product of three Coulomb waves for the final state [6]. They expressed the transition matrix element T_{fi} as the sum of three amplitudes, T_1, T_2 and T_3, which represent, respectively, the initial scattering of the incoming electron with the active electron, the nucleus and the passive electron of the helium atom. In their

paper [2], they explained that, in order for both the real and imaginary part of T_{fi} to be zero, the three amplitudes have to destructively interfere and that the amplitude T_3 is essential for a zero. Since for electron-hydrogen ionization the term $T_3 = 0$, as there is no passive electron in the target atom, Berakdar and Briggs [2] deduced that there cannot be an exact zero in T_{fi} and thus in the TDCS. Nevertheless, as pointed out by Berakdar and Briggs [2], Berakdar and Klar [7] obtained a dip in the TDCS for positron-hydrogen ionization. Also, recently, Navarrete et al. [8] and Navarrete and Barrachina [9–11], using for the final state the correlated three Coulomb wave (C3) wave function, have established that there are zeros in the transition matrix element for positron-hydrogen ionization, whereas, of course, there is also no passive electron. So, there exists the open question of whether it is possible to have zeros in the transition matrix element and the TDCS for hydrogen ionization by electron impact as well as by positron impact.

We apply the Coulomb–Born (CB1) [12–15] and modified CB1 [13,16] approximations to both positron- and electron-impact ionization of atomic hydrogen to see if we find a zero in the CB1 transition matrix $T^{\rm CB1}_{\mathbf{k},1s}$ [17–20]. We consider direct ionization (breakup) by positron impact only and, thus, we do not consider positronium formation into the continuum [21,22]. Electron-hydrogen ionization and positron-hydrogen ionization are fundamental three-body Coulomb processes. An exact zero in the ionization transition matrix element means that there is a deep minimum in the TDCS and a corresponding vortex in the velocity field, $\mathbf{v}$, associated with this element [5,18,19,23–27]. A significant advantage of the CB1 method over more sophisticated methods is that CB1 calculations can be performed rapidly, enabling a systematic search for zeros in T_{fi} to be done quickly and for the velocity field $\mathbf{v}$ associated with T_{fi} to be readily computed. Once a zero in $T^{\rm CB1}_{\mathbf{k},1s}$ and in the corresponding TDCS is located, more elaborate methods can be applied for the kinematics, or approximately the kinematics, of the zero in $T^{\rm CB1}_{\mathbf{k},1s}$. In addition to applying the CB1 and various modified CB1 approximations to electron-hydrogen ionization, we also apply the three body distorted wave (3DW) approximation and the time-dependent close-coupling (TDCC) method to electron-hydrogen ionization at incident energies close to where we obtained a zero in $T^{\rm CB1}_{\mathbf{k},1s}$.

The 3DW and TDCC methods have earlier been applied for electron-impact ionization of atomic hydrogen, molecular hydrogen and helium [28]. For the kinematics considered in reference [28], minima in the TDCSs for electron-impact ionization of atomic hydrogen were obtained, but these minima are not deep or zero. However, the TDCC [28] method obtained a deep minimum in the TDCS for electron-helium ionization for an incident energy of 64.6 eV that compared very well with experimental measurements [4]. (This incident energy of 64.6 eV is about three times the binding energy of helium.) The 3DW TDCS for the incident energy of 64.6 eV shows only a dip, although it does give a strong minimum for the incident energies of 44.6 and 54.6 eV [28]. Also, in the region of the experimental data [4], the CB1 and modified CB1 TDCSs for electron-helium ionization compared reasonably well with the measurements and with the TDCC results [25,28].

Previously, the CB1 approximation has been applied to electron-impact ionization of a K-shell model carbon atom at a high energy of 1801.2 eV [24]. A deep minimum in the CB1 TDCS and a zero in $T^{\rm CB1}_{\mathbf{k},1s}$ was obtained. Corresponding to the zero in $T^{\rm CB1}_{\mathbf{k},1s}$ there is vortex in the velocity field associated with this element [24].

For positron-hydrogen ionization a deep minimum in the fully differential cross section has previously been explained in terms of a vortex in the generalized velocity field $\mathbf{u}$ that is associated with the transition matrix element $T(\mathbf{k}_+, \mathbf{k}_-)$, where $T(\mathbf{k}_+, \mathbf{k}_-)$ depends on the momentum of the scattered positron $\mathbf{k}_+$ and the momentum of the ejected electron $\mathbf{k}_-$ [8,9]. Navarrete and Barrachina [9–11] obtained zeros in $T(\mathbf{k}_+, \mathbf{k}_-)$ and found that the velocity field rotates in opposite directions around the zeros. Recently, a deep minimum in the TDCS for positron-helium ionization was obtained using the CB1 and modified CB1 approximations [18–20,25–27].

Positron-impact ionization of atoms and molecules is of experimental interest [29–35], including studies of differential cross sections [36,37]. Structures in differential cross sections are of both theoretical and experimental interest [38].

In this paper we show that the CB1 and modified CB1 approximations give a deep minimum in the TDCS in the doubly symmetric geometry [4] for ionization of atomic hydrogen by both electron and positron impact. For electron impact the incident energy is about six times the binding energy, whereas for positron impact the incident energy is approximately seven times the binding energy. We determine the velocity field $\mathbf{v}$ associated with $T^{\rm CB1}_{\mathbf{k},1s}$ for both projectiles and notice that there is a vortex in this field which is seen by the swirling of the field around a zero in $T^{\rm CB1}_{\mathbf{k},1s}$. We are not able to compare our results with Navarrete and Barrachina's results [9–11] since they used collinear geometry and we used the doubly symmetric out-of-plane geometry.

We compare for electron-impact ionization of hydrogen the CB1, various modified CB1, 3DW and the TDCC TDCSs. This comparison is valuable since the CB1 approximation, a distorted-wave approximation, is perturbative and is applicable at high energies, while the TDCC method is an ab-initio method that is typically applied at low to intermediate energies. The CB1 gives the correct asymptotic limit for the ionization amplitude for fixed scattering angle. However, the CB1 TDCS multiplied by the modulus squared of the normalization factor of the Coulomb wave function of the two outgoing electrons gives the correct behavior in the vicinity of the Wannier's threshold law [13]. This approximation that obtains the TDCS as the product of the CB1 and the modulus squared of the normalization factor is called as the improved final-state Coulomb–Born approximation (ICBA) [13], and it is one of the three modified Coulomb–Born (CB1) approximations given in reference [16]. Surprisingly, the 3DW method, while a perturbative method, can give results that are good all the way down close to threshold, depending on the final-state energy. Since the 3DW has the post collision interaction (PCI) to all orders of perturbation theory, the 3DW can work well for intermediate to low energies, depending on the strength of the PCI [39,40].

The outline of the paper is as follows. In Section 2 we briefly describe the CB1, various modified CB1, the 3DW and the TDCC methods. We also give the expression for the velocity field $\mathbf{v}$ associated with $T^{\rm CB1}_{\mathbf{k},1s}$ and the equation of the circulation Γ. In Section 3.1 we compare for electron-hydrogen ionization the TDCS computed with the various methods. We also show $T^{\rm CB1}_{\mathbf{k},1s}$ and direction of the velocity field $\hat{\mathbf{v}} = \mathbf{v}/|\mathbf{v}|$. In Section 3.2 we present for positron-hydrogen ionization the TDCS computed with the CB1 and modified CB1 approximations and we show both $T^{\rm CB1}_{\mathbf{k},1s}$ and the direction of the velocity field.

We use atomic units throughout the paper unless otherwise stated. We report angles in degrees and the incident energies in eV.

2. Theory

The CB1 transition matrix element $T^{\rm CB1}_{\mathbf{k},1s}$, derived by Botero and Macek [12–15], is the first non-zero term in a perturbative expansion of the exact transition matrix element. For electron-impact ionization from atomic hydrogen, the direct $T^{\rm CB1}_{\mathbf{k},1s}$ is given by [12–15]

$$T^{\rm CB1}_{\mathbf{k},1s} = \langle \psi^-_{\mathbf{K}_f}(\mathbf{r})\psi^-_{\mathbf{k}}(\mathbf{r}')\left|\frac{1}{|\mathbf{r}-\mathbf{r}'|}\right|\varphi_i(\mathbf{r}')\psi^+_{\mathbf{K}_i}(\mathbf{r})\rangle, \tag{1}$$

where $\mathbf{k}$, $\mathbf{K}_i$ and $\mathbf{K}_f$ are the momentum of the ejected electron, the momentum of the incident particle, and momentum of the scattered particle, respectively. In Equation (1) $\mathbf{r}$ and $\mathbf{r}'$ are, respectively, the position vector of the incident (or scattered) particle and of the atomic (or ejected) electron relative to the proton. Also, in this equation, φ_i is the ground-state wave function of hydrogen and $\psi^{\pm}$ are Coulomb wave functions where the subscript $-$ and the subscript $+$ refer to incoming and outgoing boundary conditions, respectively [14,16].

For the doubly symmetric geometry [3,4,41] and for the effective charge $Z_{\rm eff}$ in the Coulomb wave functions of the incident electron and the scattered electron equal to the atomic number $Z_T = 1$ of

hydrogen, the direct and exchange CB1 transition matrix elements are equal. Therefore, the CB1 TDCS for electron-hydrogen ionization can be expressed as:

$$\frac{d^3\sigma^{\mathrm{CB1}}}{d\Omega_f dE_{\mathbf{k}} d\Omega_{\mathbf{k}}} = (2\pi)^4 \frac{K_f k}{K_i} |T^{\mathrm{CB1}}_{\mathbf{k},1s}|^2, \tag{2}$$

where $d\Omega_{\mathbf{k}}$ is the solid angle for the ejected electron, $d\Omega_f$ is the solid angle for the scattered particle, and $E_{\mathbf{k}}$ is the energy of the ejected electron [14,24].

The modified CB1 TDCS for electron-impact ionization is the CB1 TDCS multiplied by the normalization factor given by reference [16], namely

$$|D_3^-(\mathbf{r}_{3ave})|^2 = \frac{\pi \exp(-\frac{\pi}{k_3})}{k_3[1-\exp(-\frac{\pi}{k_3})]} |{}_1F_1(\frac{i}{2k_3}, 1, -2ik_3 r_{3ave})|^2, \tag{3}$$

where $k_3 = |\mathbf{K}_f - \mathbf{k}|/2$. Also, $\mathbf{r}_{3ave}$ is the vector whose magnitude is the average spacing between the two outgoing electrons and whose direction is taken to be along $\hat{\mathbf{k}}_3$, $\mathbf{r}_{3ave} = r_{3ave}\hat{\mathbf{k}}_3$, which is appropriate in the Wannier region.

We follow reference [16] by considering three modified CB1 approximations which correspond to three different values of r_{3ave}, namely $r_{3ave} = 0$, $r_{3ave} = 1/k_3$ and

$$r_{3ave} = \frac{\pi^2}{16\varepsilon}\left(1 + \frac{0.627}{\pi\sqrt{\varepsilon} ln\varepsilon}\right)^2, \tag{4}$$

respectively. In Equation (4), $\varepsilon = (K_f^2 + k^2)/2$, which is the total energy of the two outgoing electrons. By taking the limit $r_{3ave} \to \infty$, $|D_3^-(\mathbf{r}_{3ave})|^2 \to 1$, the CB1 TDCS is obtained. In contrast, when $r_{3ave} = 0$, $|D_3^-(\mathbf{r}_{3ave})|^2 = |N^-_{e^-e^-}|^2$, where $N^-_{e^-e^-}$ is the normalization factor of the Coulomb wave function $\psi^-_{\mathbf{k_3}}$ of the two outgoing electrons. This modified Coulomb–Born approximation is called the ICBA in reference [13].

The modulus squared of the normalized factor of the Coulomb wave function for two outgoing particles (e^- and e^- for electron-impact ionization and e^+ and e^- for positron-impact ionization) is given by [7,13,16]

$$|N^-_{e^-e^\pm}|^2 = \frac{\pm\pi \exp(\pm\frac{\pi}{k_3})}{k_3[\exp(\pm\frac{\pi}{k_3}) - 1]}. \tag{5}$$

In an earlier paper [25], and for positron-impact ionization of hydrogen, we refer to the CB1 TDCS multiplied by $|N^-_{e^-e^\pm}|^2$ as the modified CB1 TDCS. Here, where we are considering three different modified CB1 TDCS for electron-impact ionization of hydrogen, we specify this particular modified CB1 TDCS as the modified CB1 TDCS with $r_{3ave} = 0$ to distinguish it from the other two (where $r_{3ave} = 1/k_3$ and r_{3ave} is given by Equation (4)).

For positron-impact ionization, $\mathbf{K}_i$ and $\mathbf{K}_f$ in Equations (1) and (2) are the momentum of the incident positron and the momentum of the scattered electron, respectively, and the interaction of the positron with the proton is repulsive.

Triple differential cross sections for electron-impact ionization of hydrogen are also calculated within the 3DW approximation. The 3DW approach is described in previous publications [42–44] (and references therein), so here we only present the theoretical aspects relevant to the present paper. In this approach, the wave functions for the incident electron, scattered electron, and ejected electron are all distorted waves. The important distinction of the method is that the exact final state electron-electron interaction, normally called the post collision interaction (PCI), is included in the approximation for the final state wave function of the system. The fact that any physical effect included in the system wave function is automatically included to all orders of perturbation theory means that PCI is included to all orders of perturbation theory in this approach. In the 3DW approximation the direct and exchange amplitudes are identical for the doubly symmetric in-plane geometry for electron-hydrogen ionization.

The TDCC calculations shown here are very similar to previous calculations [28] for electron ionization of atomic hydrogen. In brief, the TDCC approach solves the time-dependent Schrödinger equation for the two electrons by propagating the corresponding differential equations in time until convergence of the probabilities for ionization has been reached. The calculations shown here included fourteen partial waves, which were found to be sufficient for the TDCS calculations shown here. We note that the small cross sections found at larger scattering angles (beyond 100°) are quite sensitive to some of the numerical aspects of the calculations (such as mesh size, number of coupled channels). We note that these small cross sections are around three orders of magnitude lower than the peak of the cross section, which occurs at a scattering angle of approximately 39°.

When there is a zero in the real and imaginary parts of $T_{\mathbf{k},1s}$, there is a vortex in the velocity field associated with $T_{\mathbf{k},1s}$. Previously vortices in the velocity fields associated with atomic wave functions have been discussed by Bialynicki-Birula et al. [45]. Recently vortices in the velocity field associated with the ionization amplitude have been discussed by Macek et al. [5] and by Macek [23]. Here, we discuss vorticies in the velocity field associated with the transition matrix element which is proportional to the ionization amplitude [24]. The velocity field $\mathbf{v}$ associated with $T^{\mathrm{CB1}}_{\mathbf{k},1s}$ for electron or positron ionization can be expressed as [24,25]

$$\mathbf{v} = \nabla_{\mathbf{k}} \mathrm{Im}[\ln T^{\mathrm{CB1}}_{\mathbf{k},1s}]. \tag{6}$$

The circulation, Γ, for a closed contour, c, taken in the anticlockwise direction that encloses only one first-order zero in $T^{\mathrm{CB1}}_{\mathbf{k},1s}$ is given by [5,23–25,45]

$$\Gamma = \int_c \mathbf{v} \cdot d\ell = \pm 2\pi. \tag{7}$$

3. Results

3.1. Deep Minimum in the TDCS for Electron-Impact Ionization of Hydrogen

For electron-impact ionization of hydrogen we perform calculations for the doubly symmetric in-plane geometry (Figure 1a) where both outgoing particles have the same energy and same angle, ξ, with respect to the z-axis. This geometry was used by Murray and Reed in their experimental measurements for electron-helium ionization [4]. The scattered electron makes a polar angle with respect to the z-axis of ξ while the ejected electron makes an angle of $-\xi$ with respect to the same axis.

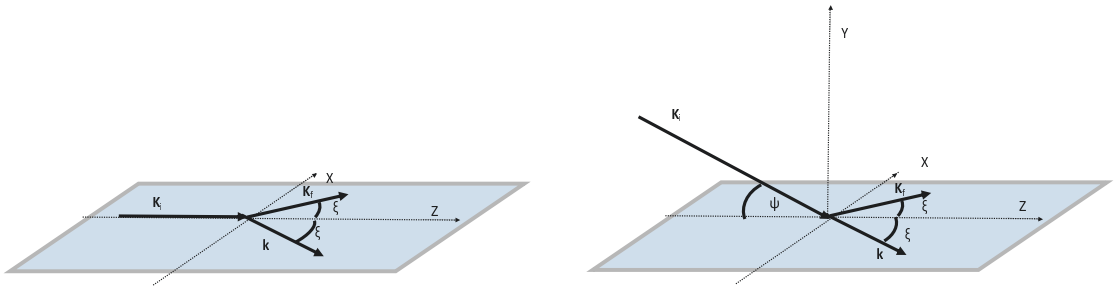

(**a**) In-Plane (**b**) Out-of-Plane

Figure 1. Geometry figures for both in-plane and out-of-plane configurations.

A deep minimum in the TDCS occurs when the real and imaginary parts of the transition matrix element, $T_{\mathbf{k},1s}$, are identically zero at the same angle; this occurs at a polar angle of 87.94° in the CB1 approximation (Figure 2). A comparison of the TDCSs computed with the CB1, modified CB1 with $r_{3ave} = 0$, modified CB1 with $r_{3ave} = 1/k_3$, and the modified CB1 with r_{3ave} given by Equation (4) approximations can be seen in Figure 3a. The position of the minimum is the same for these four approximations.

We show the comparison between the modified CB1 with $r_{3ave} = 0$, 3DW, and TDCC methods in Figure 3b. There is a dip 3DW TDCS at a polar angle of 90.2° and a slight dip in the TDCC TDCS at a polar angle of 90.6°. The polar angle for the deep minimum in the CB1 TDCS is within 3 degrees of these angles.

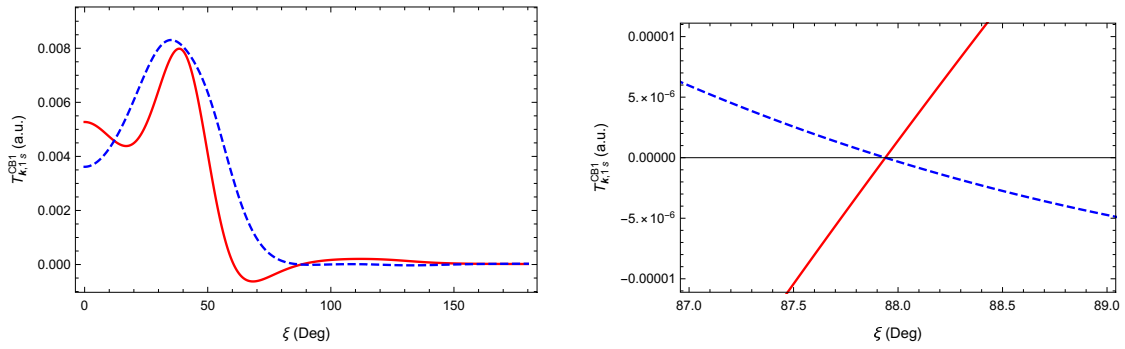

(**a**) (**b**)

Figure 2. Transition matrix element, $T^{CB1}_{\mathbf{k},1s}$, versus the polar angle ξ for electron-impact ionization of hydrogen at 76.4541 eV. (**a**) Re$[T^{CB1}_{\mathbf{k},1s}]$ (solid red line) and Im$[T^{CB1}_{\mathbf{k},1s}]$ (dashed blue line) over the full angular range (**b**) Re$[T^{CB1}_{\mathbf{k},1s}]$ (solid red line) and Im$[T^{CB1}_{\mathbf{k},1s}]$ (dashed blue line) in the vicinity of the zero in $T^{CB1}_{\mathbf{k},1s}$.

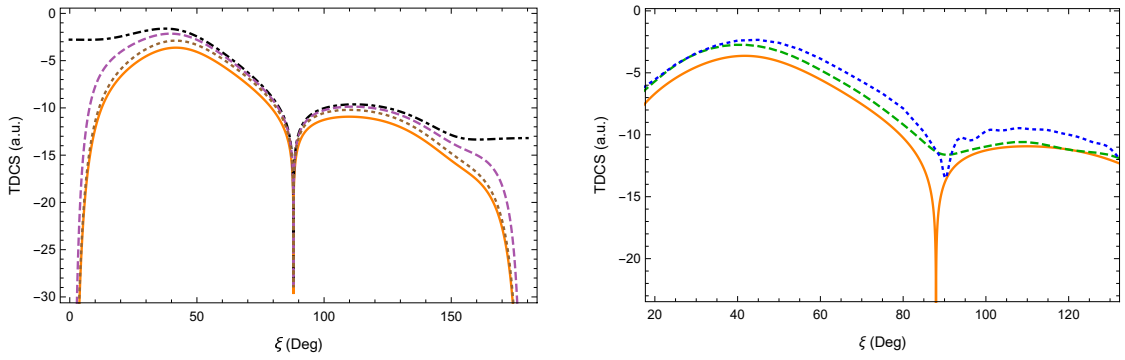

(**a**) (**b**)

Figure 3. Triply differential cross section (TDCS) on a log (ln) scale versus the polar angle ξ for electron-impact ionization of hydrogen at 76.4541 eV. (**a**) Comparison of the CB1 TDCS (dot-dashed black line), the modified CB1 TDCS with $r_{3ave} = 0$ (solid orange line), the modified CB1 TDCS with $r_{3ave} = 1/k_3$ (dashed purple line) and the modified CB1 TDCS with r_{3ave} given by Equation (4) (dotted brown line). (**b**) Comparison of the modified CB1 TDCS with $r_{3ave} = 0$ (solid orange line) with an incident energy of 76.4541 eV, the 3DW TDCS (dotted blue line) for an incident energy of 76.46 eV, and the TDCC TDCS (dashed green line) for an incident energy of 76.45 eV.

A zero in the transition matrix element means that there is a vortex in the velocity field (Figure 4) associated with this element. The rotation of the velocity field is in the anticlockwise direction and the value of the circulation Γ is 2π. Figure 4 shows the nodal lines of Re$[T^{CB1}_{\mathbf{k},1s}]$ and Im$[T^{CB1}_{\mathbf{k},1s}]$ and it shows the direction of the velocity field, $\hat{\mathbf{v}} = \mathbf{v}/|\mathbf{v}|$, by the arrows. (The axes for this figure are k_z and k_x, where k_z and k_x are respectively the z- and x-components of the momentum $\mathbf{k}$ of the ejected electron [25].) The figure also shows a density plot of $\ln|T^{CB1}_{\mathbf{k},1s}|$.

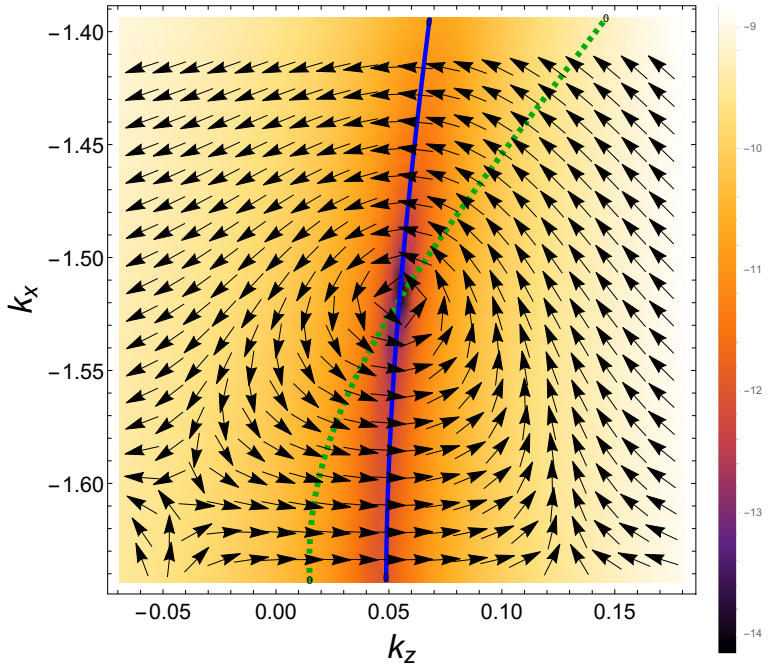

Figure 4. A density plot of $\ln|T^{\mathrm{CB1}}_{\mathbf{k},1s}|$ for electron-impact ionization of hydrogen for a fixed incident energy of 76.4541 eV in-plane and a grid in the z- and x-components of the momentum (k_z, k_x) of the ejected electron $\mathbf{k}$. The nodal lines of $\mathrm{Re}[T^{\mathrm{CB1}}_{\mathbf{k},1s}]$ and $\mathrm{Im}[T^{\mathrm{CB1}}_{\mathbf{k},1s}]$ are shown respectively, by the solid blue line and the dashed green line. The direction of the velocity field, $\hat{\mathbf{v}} = \mathbf{v}/|\mathbf{v}|$, is indicated by the arrows.

3.2. Deep Minimum in the CB1 TDCS for Positron-Impact Ionization of Hydrogen

For positron-impact ionization of hydrogen, we also consider a doubly symmetric geometry; however, for this projectile, we use the out-of-plane geometry that we show in Figure 1b. The gun angle ψ is the angle the incident particle makes with the z-axis [4]. We find a deep minimum in the CB1 TDCS for an incident energy of 100 eV with a gun angle of 56.13°. We choose this incident energy because it had been previously used [9]. Using the CB1 approximation, we vary the gun angle until we obtain a zero in $T^{\mathrm{CB1}}_{\mathbf{k},1s}$. The zero in $T^{\mathrm{CB1}}_{\mathbf{k},1s}$ can be seen in Figure 5.

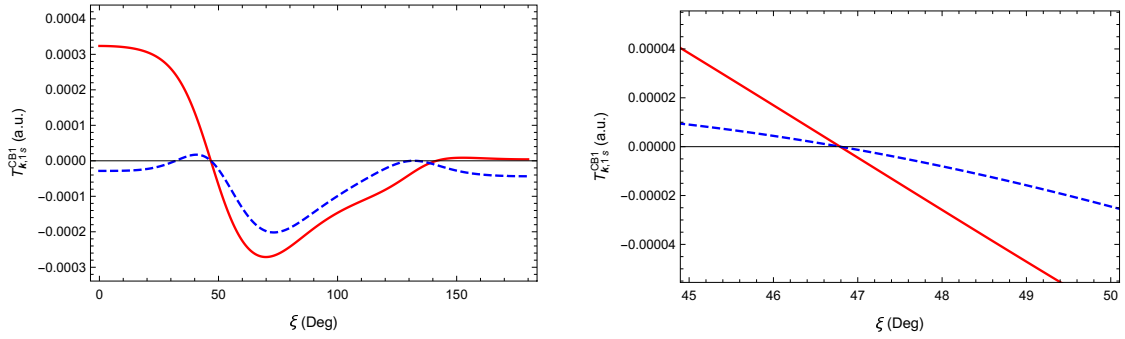

Figure 5. Transition matrix element $T^{\mathrm{CB1}}_{\mathbf{k},1s}$ versus the polar angle, ξ, for positron-impact ionization of hydrogen at 100 eV with a gun angle, ψ, of 56.13°. (**a**) $\mathrm{Re}[T^{\mathrm{CB1}}_{\mathbf{k},1s}]$ (solid red line) and $\mathrm{Im}[T^{\mathrm{CB1}}_{\mathbf{k},1s}]$ (dashed blue line) over the full angular range (**b**) $\mathrm{Re}[T^{\mathrm{CB1}}_{\mathbf{k},1s}]$ (solid red line) and $\mathrm{Im}[T^{\mathrm{CB1}}_{\mathbf{k},1s}]$ (dashed blue line) in the vicinity of the zero in $T^{\mathrm{CB1}}_{\mathbf{k},1s}$.

In the positron-impact ionization of hydrogen at 100 eV with a gun angle of 56.13° there is a deep minimum in the TDCS at a polar angle of 46.79°. This deep minima in the TDCS and a secondary dip around $\xi \approx 140°$ can be seen in Figure 6. The secondary dip in the TDCS is in the vicinity of

the intersection point of the real and imaginary parts of $T^{\mathrm{CB1}}_{\mathbf{k},1s}$ and a second zero in $\mathrm{Re}[T^{\mathrm{CB1}}_{\mathbf{k},1s}]$ (see Figure 5). We perform an out-of-plane search to see if we could find a zero in $T^{\mathrm{CB1}}_{\mathbf{k},1s}$ around $\approx 140^\circ$, but without success.

We note that we also obtain a deep minimum in the TDCS for a slightly lower incident energy, 95 eV, if the gun angle is reduced a little to 55.75°. We expect that we could track the position of the deep minimum for different incident energies and obtain a locus of points that gives the angles ψ and ξ for these energies as we did previously for electron-helium ionization [25].

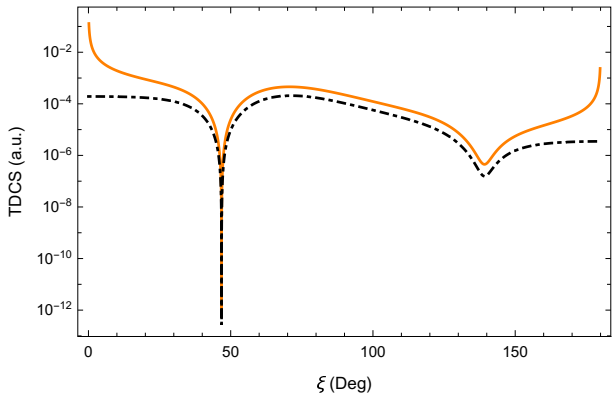

Figure 6. TDCS on a log (ln) scale versus the polar angle, ξ, for positron-impact ionization of hydrogen at 100 eV with a gun angle of 56.13°. Comparison of the CB1 TDCS (dot-dashed black line) and the modified CB1 TDCS (solid orange line) results.

For positron-impact ionization of hydrogen, we find that circulation Γ is 2π and the velocity field that is associated with the zero in $T^{\mathrm{CB1}}_{\mathbf{k},1s}$ rotates anticlockwise, as can be seen in Figure 7. This figure shows the direction of the velocity field, $\hat{\mathbf{v}} = \mathbf{v}/|\mathbf{v}|$, by the arrows and it shows the nodal lines of $\mathrm{Re}[T^{\mathrm{CB1}}_{\mathbf{k},1s}]$ and $\mathrm{Im}[T^{\mathrm{CB1}}_{\mathbf{k},1s}]$. It also gives a density plot of $\ln|T^{\mathrm{CB1}}_{\mathbf{k},1s}|$.

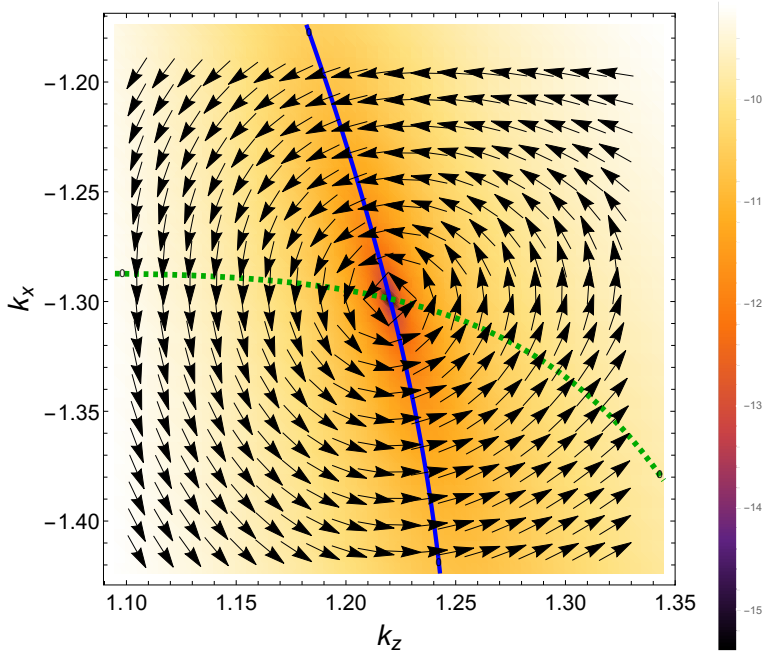

Figure 7. A density plot of $\ln|T^{\mathrm{CB1}}_{\mathbf{k},1s}|$ for positron-impact ionization of hydrogen for a fixed incident energy of 100 eV out-of-plane with a gun angle of 56.13° and a grid in the z- and x-components of the momentum (k_z, k_x) of the ejected electron $\mathbf{k}$. The nodal lines of $\mathrm{Re}[T^{\mathrm{CB1}}_{\mathbf{k},1s}]$ and $\mathrm{Im}[T^{\mathrm{CB1}}_{\mathbf{k},1s}]$ are shown respectively, by the solid blue line and the dashed green line. The direction of the velocity field, $\hat{\mathbf{v}} = \mathbf{v}/|\mathbf{v}|$, is indicated by the arrows.

For the specific geometries and kinematics that we consider, the direction of rotation of the velocity field is the same for positron- and electron-impact ionization of hydrogen. Interestingly, for the two ionization processes, the polar angle ξ of the deep minimum in the CB1 TDCS is less than 90°, and thus, ξ lies in the first quadrant.

4. Conclusions

While a deep minimum in the TDCS was not expected to exist for electron-impact ionization of hydrogen, we were able to obtain one using the CB1 and modified CB1 approximations for an incident energy of 76.4541 eV [2]. The CB1 approximation is a high-energy approximation that has been applied to intermediate energies. Previously, the CB1 and modified CB1 approximations have been applied to electron-helium ionization for an incident energy of 64.6 eV [25]; and, in the region of the experimental data, the TDCS results compare reasonably well with experimental measurements [4] and with TDCC results [28]. These approximations have also been applied previously to positron-helium ionization [25].

Using the CB1 and a modified CB1 approximations we obtain a deep minimum in the TDCS for positron-impact ionization of hydrogen for an incident energy of 100 eV in the doubly symmetric out-of-plane geometry with a gun angle of 56.13°. This energy has been previously considered for positron-hydrogen ionization in the collinear geometry [8,9]. A benefit of the CB1 approximation is that it is a fairly simple approximation that does not take much computing time.

While the question of whether there can be a zero in the transition matrix element and a corresponding deep minimum in the TDCS for electron-impact ionization of hydrogen has not been resolved, we have found that these exist within the CB1 approximation. Due to the fact that zeros in a transition matrix element have been found previously for positron-impact ionization of hydrogen [8,9], a zero in $T^{\mathrm{CB1}}_{\mathbf{k},1s}$ for electron-hydrogen ionization is not that surprising even though there is no passive electron. We note that, for electron-hydrogen ionization, neither the TDCC or 3DW methods obtained a deep minimum in the TDCS; however, they did obtain a dip.

The direction of the rotation of the velocity field around a zero in $T^{\mathrm{CB1}}_{\mathbf{k},1s}$ does not appear to be projectile dependent as for both electron- and positron-impact ionization of hydrogen the rotation is anticlockwise. This may be due to the fact that the polar angle of the zero in $T^{\mathrm{CB1}}_{\mathbf{k},1s}$ is between 0° and 90° (first quadrant) for both cases. An earlier paper shows, for positron-helium ionization, clockwise rotation of the velocity field about the zero in $T^{\mathrm{CB1}}_{\mathbf{k},1s}$; however, the polar angle for this zero is between 90° and 180° (second quadrant) [25]. For the energies that were considered in reference [25] for electron-helium ionization the direction of the velocity field is anticlockwise and the polar angle lies in the first quadrant.

The interesting finding that for both electron- and positron-impact ionization of hydrogen the velocity field rotates in the same direction is different from the previous finding for impact ionization of helium [25]. This may be due to the fact that for impact ionization of hydrogen by the two projectiles the deep minimum in the TDCS occurs at an angle less than 90°, while for earlier results of electron and positron ionization of helium the zeros occur in different quadrants [25].

Author Contributions: C.M.D. and S.J.W. prepared the manuscript (with input from J.C. and D.H.M.). C.M.D., under the supervision of S.J.W., performed the CB1 and modified CB1 calculations for both electron- and positron-impact ionization of hydrogen. J.C. performed the TDCC calculations and provided a discussion of the method. The 3DW calculations are from D.H.M. and S.A. A discussion on the 3DW approximation was provided by D.H.M. All authors have read and agreed to the published version of the manuscript.

Funding: S.J.W. is thankful for support from the NSF under Grant No. PHYS-1707792.

Acknowledgments: J. B. Kent, while an undergraduate student at UNT and under the supervision of S. J. Ward, performed CB1 and modified CB1 calculations for electron-impact ionization of hydrogen. We acknowledge that, for electron-hydrogen ionization, he was the first to locate the position of the zero in the CB1 transition matrix element and the corresponding deep minimum in the TDCS. SJW would like to thank Gaetana (Nella) Laricchia for encouraging the CB1 investigation. CMD and SJW are thankful for the CB1 Fortran codes from Javier Botero. Wolfram Research [46] and Microsoft Publisher [47] were used to generate the images in this paper. Also, Wolfram Research [46] was used in some of the calculations. JC acknowledges the support by the US Department of Energy

through the ASC PEM Program of the Los Alamos National Laboratory. Los Alamos National Laboratory is operated by Triad National Security, LLC, for the National Nuclear Security Administration of U.S. Department of Energy (Contract No. 89233218CNA000001).

Conflicts of Interest: The authors declare no conflict of interest.

Abbreviations

The following abbreviations are used in this manuscript:

MDPI	Multidisciplinary Digital Publishing Institute
DOAJ	Directory of open access journals
TDCS	Triply differential cross section
CB1	Coulomb–Born
TDCC	Time-dependent close-coupling
3DW	Three body distorted wave

References

1. Briggs, J.S. Cusps, dips and peaks in differential cross-sections for fast three-body Coulomb collisions. *Comments At. Mol. Phys.* **1989**, *23*, 155–174.
2. Berakdar, J.; Briggs, J.S. Interference effects in (e,2e)-differential cross sections in doubly symmetric geometry. *J. Phys. B At. Mol. Opt. Phys.* **1994**, *27*, 4271–4280. [CrossRef]
3. Murray, A.J.; Read, F.H. Exploring the helium (e,2e) differential cross section at 64.6 eV with symmetric scattering angles but non-symmetric energies. *J. Phys. B At. Mol. Opt. Phys.* **1993**, *26*, L359–L365. [CrossRef]
4. Murray, A.J.; Read, F.H. Evolution from the coplanar to the perpendicular plane geometry of helium (e,2e) differential cross sections symmetric in scattering angle and energy. *Phys. Rev. A* **1993**, *47*, 3724–3732. [CrossRef] [PubMed]
5. Macek, J.H.; Sternberg, J.B.; Ovchinnikov, S.Y.; Briggs, J.S. Theory of deep minima in (e,2e) measurements of triply differential cross sections. *Phys. Rev. Lett.* **2010**, *104*, 033201. [CrossRef]
6. Berakdar, J.; Briggs, J.S. Three-body Coulomb continuum problem. *Phys. Rev. Lett.* **1994**, *72*, 3799–3802. [CrossRef] [PubMed]
7. Berakdar, J.; Klar, H. Structures in triply and doubly differential ionization cross sections of atomic hydrogen. *J. Phys. B At. Mol. Opt. Phys.* **1993**, *26*, 3891–3913 [CrossRef]
8. Navarrete, F.; Picca, R.D.; Fiol, J.; Barrachina, R.O. Vortices in ionization collisions by positron impact. *J. Phys. B At. Mol. Opt. Phys.* **2013**, *46*, 115203. [CrossRef]
9. Navarrete, F.; Barrachina, R.O. Vortices in the three-body electron-positron-proton continuum system induced by the positron-impact ionization of hydrogen. *J. Phys. B At. Mol. Opt. Phys.* **2015**, *48*, 055201. [CrossRef]
10. Navarrete, F.; Barrachina, R.O. Vortices in ionization collisions. *Nucl. Instrum. in Phys. Res. B* **2016**, *369*, 72–76. [CrossRef]
11. Navarrete, F.; Barrachina, R.O. Vortex rings in the ionization of atoms by positron impact. *J. Phys. B Conf. Ser.* **2017**, *875*, 012022. [CrossRef]
12. Botero, J.; Macek, J.H. Coulomb Born approximation for electron scattering from neutral atoms: Application to electron impact ionization of helium in coplanar symmetric geometry. *J. Phys. B At. Mol. Opt. Phys.* **1991**, *24*, L405–L411. [CrossRef]
13. Botero, J.; Macek, J.H. Threshold angular distributions of (e, 2e) cross sections of helium atoms. *Phys. Rev. Lett.* **1992**, *68*, 576–579. [CrossRef] [PubMed]
14. Botero, J.; Macek, J.H. Coulomb-Born calculation of the triple-differential cross section for inner-shell electron-impact ionization of carbon. *Phys. Rev. A* **1992**, *45*, 154–165. [CrossRef] [PubMed]
15. Macek, J.H.; Botero, J. Perturbation theory with arbitrary boundary conditions for charged-particle scattering: Application to (e,2e) experiments in helium. *Phys. Rev. A* **1992**, *45*, R8. [CrossRef]
16. Ward, S.J.; Macek, J.H. Wave functions for continuum states of charged fragments. *Phys. Rev. A* **1994**, *49*, 1049–1056. [CrossRef]

17. Ward, S.J.; Kent, J.B. Deep minimum in the Coulomb-Born TDCS for electron-impact ionization of atomic hydrogen. *Bull. Am. Phys. Soc.* **2017**, *62*, 28. Available online: http://meetings.aps.org/link/BAPS.2017.GEC.GT1.1 (accessed on 25 May 2020).
18. Ward, S.J. Vortices for Positron Ionization and Positronium Formation. Available online: http://meetings.aps.org/Meeting/GEC19/Session/LW1.6 (accessed on 25 May 2020).
19. DeMars, C.M.; Kent, J.B.; Ward, S.J. Abstract: Q01.00026: Deep Minima in the Coulomb-Born Triply Differential Cross Section for Electron and Positron Ionization of Hydrogen and Helium. Available online: https://meetings.aps.org/Meeting/DAMOP20/Session/Q01.26 (accessed on 25 May 2020).
20. DeMars, C.M.; Ward, S.J.; Kent, J.B. Deep Minima in the Coulomb-Born triply differential cross section for electron and positron ionization of hydrogen and helium. Submitted May 2020 to GEC 2020.
21. Kadyrov, A.S.; Bray, I.; Stelbovics, A.T. Near-threshold positron-impact ionization of atomic hydrogen. *Phys. Rev. Lett.* **2007**, *98*, 263202. [CrossRef]
22. Kadyrov, A.S.; Bray, I. Recent progress in the description of positron scattering from atoms using the convergent close-coupling theory. *J. Phys. B At. Mol. Opt. Phys.* **2016**, *49*, 22202. [CrossRef]
23. Macek, J.H. Vortices in atomic processes. In *Dynamical Processes in Atomic and Molecular Physics*; Ogurtsov, G., Dowek, D., Eds.; Bentham Science: Sharjah, UAE, 2012; Chapter 1, pp. 3–28.
24. Ward, S.J.; Macek, J.H. Effect of a vortex in the triply differential cross section for electron impact K-shell ionization of carbon. *Phys. Rev. A* **2014**, *90*, 062709. [CrossRef]
25. DeMars, C.M.; Kent, J.B.; Ward, S.J. Deep minima in the Coulomb-Born triply differential cross sections for ionization of helium by electron and positron impact. *Eur. Phys. J. D* **2020**, *74*, 48.
26. DeMars, C.M.; Kent, J.B.; Ward, S.J. Deep minimum in the Coulomb-Born TDCS for e^--He and e^+-He ionization. *Bull. Am. Phys. Soc.* **2019**, *64*, 119. Available online: http://meetings.aps.org/Meeting/DAMOP19/Session/L01.13 (accessed on 25 May 2020).
27. DeMars, C.M.; Ward, S.J. Deep minima in the TDCS for positron-helium ionization computed using the Coulomb-Born approximation. In *Proceedings of the XX International Workshop on Low-Energy Positron and Positronium Physics* (POSMOL 2019 Book of Abstracts), Belgrade, Serbia, 18–21 July 2019; Cassidy, D., Brunger, M.J., Petrovíc, Z.L., Dujko, S., Marinković, B.P., Maríc, D., Tošić, S., Eds.; Serbian Academy of Sciences and Arts: Belgrade, Serbia, 2019; LEPPP 12, p. 53. Available online: http://posmol2019.ipb.ac.rs/_files/Book_POSMOL2019_Online.pdf (accessed on 25 May 2020).
28. Colgan, J.; Al-Hagan, O.; Madison, D.H.; Murray, A.J.; Pindzola, M.S. Deep interference minima in non-coplanar triple differential cross sections for the electron-impact ionization of small atoms and molecules. *J. Phys. B At. Mol. Opt. Phys.* **2009**, *42*, 171001.
29. Jones, G.O.; Charlton, M.; Slevin, J.; Laricchia, G.; Kövér, Á.; Poulsen, M.R.; Chormaic, S.N. Positron impact ionization of atomic hydrogen. *J. Phys. B At. Mol. Opt. Phys.* **1993**, *26*, L483–L488. [CrossRef]
30. Murtagh, D.J.; Szłuińska, M.; Moxom, J.; Reeth, P.V.; Laricchia, G. Positron-impact ionization and positronium formation from helium. *J. Phys. B At. Mol. Opt. Phys.* **2005**, *38*, 3857–3866. [CrossRef]
31. Laricchia, G.; Brawley, S.; Cooke, D.A.; Kövér, Á.; Murtagh, D.J.; Williams, A.I. Ionization in positron- and positronium-collisions with atoms and molecules. *J. Phys. Conf. Ser.* **2009**, *194*, 012036.
32. Laricchia, G.; Cooke, D.A.; Köver, A.; Brawley, S.J. Experimental aspects of ionization studies by positron and positronium impact, In *Fragmentation Processes: Topics in Atomic and Molecular Physics*; Whelan, C.T., Ed.; Cambridge University Press: Cambridge, UK, 2013; Chapter 5, pp. 116–136.
33. DuBois, R.D. Topical Review, Methods and progress in studying inelastic interactions between positrons and atoms. *J. Phys. B At. Mol. Opt. Phys.* **2016**, *49*, 112002. [CrossRef]
34. Surko, C.M.; Gribakin, G.F.; Buckman, S.J. Topical Review, Low-energy positron interactions with atoms and molecules. *J. Phys. B At. Mol. Opt. Phys.* **2005**, *38*, R57–R126. [CrossRef]
35. Schippers, S.; Sokell, E.; Aumayr, F.; Sadeghpour, H.; Ueda, K.; Bray, I.; Bartschat, K.; Murray, A.; Tennyson, J.; Dorn, A.; et al. Roadmap on photonic, electronic and atomic collisions: II. Electron and antimatter interactions. *J. Phys. B At. Mol. Opt. Phys.* **2019**, *52*, 171002. [CrossRef]
36. Kövér, Á.; Laricchia, G. Triply differential study of positron impact ionization of H_2. *Phys. Rev. Lett.* **1998**, *80*, 5309–5312.
37. Kövér, Á.; Murtagh, D.J.; Williams, A.I.; Laricchia, G. Differential ionization studies by positron impact. *J. Phys. Conf. Ser.* **2010**, *199*, 012020. [CrossRef]

38. Navarrete, F.; Feole, M.; Barrachina, R.O.; Kövér, Á. When vortices and cusps meet. *J. Phys. Conf. Ser.* **2015**, *583*, 01202. [CrossRef]
39. Ali, E.; Ren, X.; Dorn, A.; Ning, C.; Colgan, J.; Madison, D.H. Experimental and theoretical triple-differential cross sections for tetrahydrofuran ionized by low-energy 26-eV-electron impact. *Phys. Rev. A* **2016**, *93*, 062705. [CrossRef]
40. Ali, E.; Chakraborty, H.S.; Madison, D.H. Improved theoretical calculations for electron-impact ionization of DNA analogue molecules. *J. Chem. Phys.* **2020**, *152*, 124303. [CrossRef] [PubMed]
41. Murray, A.J.; Read, F.H. Novel exploration of the helium (e,2e) ionization processes. *Phys. Rev. Lett.* **1992**, *69*, 2912–2914. [CrossRef] [PubMed]
42. Jones, S.; Madison, D.H.; Franz, A.; Altick, P.L. Three-body distorted-wave Born approximation for electron-atom ionization. *Phys. Rev. A* **1993**, *48* R22–R25. [CrossRef]
43. Jones, S.; Madison, D.H. Ionization of hydrogen atoms by fast electrons. *Phys. Rev. A* **2000**, *62*, 042701.
44. Madison, D.H.; Al-Hagan, O. The distorted-wave Born approach for calculating electron-impact ionization of molecules. *J. At. Mol. Opt. Phys.* **2010**, *2010*, 367180.
45. Bialynicki-Birula, I.; Bialynicka-Birula, Z.; Śliwa, C. Motion of vortex lines in quantum mechanics. *Phys. Rev. A* **2000**, *61*, 032110. [CrossRef]
46. Wolfram Research, Inc. *Mathematica*; Version 11.3; Wolfram Research, Inc.: Champaign, IL, USA, 2018.
47. Microsoft Office 365 ProPlus. Available online: https://www.microsoft.com/en-us/microsoft-365/publisher (accessed on 25 May 2020).